

# Pole analysis on the doubly charmed meson in $D^0 D^0 \pi^+$ mass spectrum

Ling-Yun Dai<sup>1,2,\*</sup>, Xiang Sun<sup>1,2</sup>, Xian-Wei Kang<sup>3,4</sup>, A. P. Szczepaniak<sup>5,6,7,†</sup> and Jie-Sheng Yu<sup>1,2‡</sup>

<sup>1</sup>*School of Physics and Electronics, Hunan University, Changsha 410082, China*

<sup>2</sup>*Hunan Provincial Key Laboratory of High-Energy Scale Physics and Applications, Hunan University, Changsha 410082, China*

<sup>3</sup>*Key Laboratory of Beam Technology of the Ministry of Education, College of Nuclear Science and Technology, Beijing Normal University, Beijing 100875, China*

<sup>4</sup>*Beijing Radiation Center, Beijing 100875, China*

<sup>5</sup>*Physics Department, Indiana University, Bloomington, IN 47405, USA*

<sup>6</sup>*Center for Exploration of Energy and Matter, Indiana University, Bloomington, IN 47403, USA*

<sup>7</sup>*Thomas Jefferson National Accelerator Facility, Newport News, VA 23606, USA*

In this paper we study the scattering amplitudes of  $D^0 D^0 \pi^+ - D^{*+} D^0$  coupled channels based on  $K$ -matrix within the Chew-Mandelstam formalism. The  $D^0 D^0 \pi^+$  invariant mass spectrum of LHCb is fitted and the pole parameters of the  $T_{cc}^+$  are extracted. The analysis of pole behavior suggests that the  $T_{cc}^+$  may originate from a  $D^{*+} D^0$  virtual state and is formed as a result of an interplay between an attractive interaction between  $D^0$  and  $D^{*+}$  and coupling to  $D^0 D^0 \pi^+$  channel.

*Introduction.*— For over half a century the quark model served as the fundamental template for constructing hadrons. [1–3]. Dozens of known hadrons can be classified according to this model with three quarks in a baryon and a quark-antiquark pair in a meson. However, the requirement of color neutrality alone does not preclude existence of more complicated structures, including, for example tetraquarks and pentaquarks. In the last twenty years several candidates for such multi-quark hadrons, specifically containing heavy quarks, have been observed by the Belle, BaBar, BESIII, D0, CDF, CMS, and LHCb experiments [4–14]. Significant number of these states are found lying close to various thresholds for decays into non-exotic hadrons. For example the  $X(3872)$  discovered by Belle [4] is in a mass region that is not expected to host a quark model-like charmonium state, but it is only  $\sim 1$  MeV away from the  $D\bar{D}^*$  threshold. Proximity to this threshold makes it likely to be a  $D\bar{D}^*$  molecule [15–17]. Recently, the LHCb Collaboration announced observation of another  $X$ -like candidate, this time however, containing two charm quarks instead of a charm-anti-charm pair, labeled  $T_{cc}$  [18, 19]. The  $T_{cc}$  was observed, with a  $21.7\sigma$  significance, in the  $D^0 D^0 \pi^+$  invariant mass spectrum near threshold, *aka.* with the mass close to the  $X(3872)$ ,  $M_{T_{cc}^+} - (M_{D^{*+}} + M_{D^0}) = -237 \pm 61$  keV/ $c^2$  and width,  $\Gamma_{T_{cc}^+} = 410 \pm 165$  keV. Because two charm quarks alone cannot form a color singlet hadron, if confirmed, the  $T_{cc}$  would be a clear evidence of a multi-quark hadron. The small width indicates that there could be a pole in the relevant partial wave close to the  $D^0 D^{*+}$  threshold. However, since  $D^*$  decays to  $D\pi$ , rescattering between  $D^0 D^0 \pi^+$  and  $D^0 D^{*+}$  should be taken into account in determining the pole parameters [20–25].

In this note we use effective range approximation and consider the coupled amplitudes for production of  $D^0 D^0 \pi^+$  and  $D^{*+} D^0$  final states. By fitting to the line shape we obtain a solution for the production amplitude which enables analytical continuation to the complex energy plane where we extract the pole parameters. Finally, by analyzing the pole position we speculate on the possible nature of the  $T_{cc}$  peak.

*Formalism.*— We need analytical amplitudes to de-

scribe the  $D^0 D^0 \pi^+$  invariant mass spectrum in order to obtain accurate pole information. The  $T_{cc}^+$  is found in the  $D^0 D^0 \pi^+$  invariant mass spectrum near the  $D^{*+} D^0$  threshold of 3875.09 MeV. One also notices that the branching ratio of  $D^{*+} \rightarrow D^0 \pi^+$  is  $67.7 \pm 0.5\%$  [26]. Hence it is natural to consider the  $D^0 D^0 \pi^+ - D^0 D^{*+}$  coupled channels. The analytical coupled channel amplitudes near threshold can be parametrized using a real, symmetric  $2 \times 2$   $K$ -matrix to describe the analytical part of the inverse amplitudes,

$$T^{-1}(s) = K^{-1}(s) - C(s), \quad (1)$$

The matrix elements  $C_i(s)$  of the diagonal  $2 \times 2$  Chew-Mandelstam (CM) function [27–29],  $C(s) = C_i(s)\delta_{i,j}$  contain the right hand cuts starting at the thresholds,  $s_{th,i} = (M_i + m_i)^2$ . Here the masses are  $M_1 = M_{D^0} + m_{\pi^+}$ ,  $m_1 = M_{D^0}$ , and  $M_2 = M_{D^{*+}}$ ,  $m_2 = M_{D^0}$  for the  $D^0 D^0 \pi^+$  and  $D^0 D^{*+}$  channels, respectively. Note that the  $D^0 \pi^+$  system is treated as an isobar of spin-1 and therefore the amplitude  $T$  describes spin-0 partial waves. The CM function,

$$C_i(s) = \frac{s}{\pi} \int_{s_{th,i}}^{\infty} ds' \frac{\rho_i(s')}{s'(s' - s)}, \quad (2)$$

is defined by the (quasi)two-body  $S$ -wave phase space factor,  $ImC_i(s) = \rho_i(s) = \lambda^{1/2}(s, M_i^2, m_i^2)/s$ , explicitly,

$$C_i(s; M_i, m_i) = \left[ \frac{M_i^2 - m_i^2}{\pi s} - \frac{M_i^2 + m_i^2}{\pi(M_i^2 - m_i^2)} \right] \ln \left( \frac{m_i}{M_i} \right) + \frac{1}{\pi} + \frac{\rho_i(s)}{\pi} \ln \left( \frac{\sqrt{s_{th,i}} - s - \sqrt{(M_i - m_i)^2 - s}}{\sqrt{s_{th,i}} - s + \sqrt{(M_i - m_i)^2 - s}} \right). \quad (3)$$

With the threshold singularities accounted for by  $C(s)$ , the  $K$ -matrix is analytical in the vicinity at thresholds and in the effective range approximation it is approximated by a matrix of constants.

In the notation of [30, 31] the  $s$ -dependence of production amplitude for the processes  $pp \rightarrow D^0 D^0 \pi^+ + X$

and  $pp \rightarrow D^0 D^{*+} + X$ , can be represented by a two-dimensional vector

$$F_i(s) = \sum_{k=1}^2 \alpha_k(s) T_{ki}(s). \quad (4)$$

where  $\alpha_i(s)$  are regular functions of  $s$  on the physical cut. Since the range of invariant mass is small, with  $\Delta\sqrt{s} \ll O(100 \text{ MeV})$ , we can safely ignore any variation in  $s$  of the production amplitudes,  $\alpha_i(s)$  and also approximate them by constants. Finally, the measured yield is proportional to the differential cross section and given by

$$\frac{dY_1}{d\sqrt{s}} = N p_1 |F_1|^2. \quad (5)$$

Here  $p_1 = \lambda(s, M_1^2, m_1^2)/2\sqrt{s}$  is the magnitude of the momentum of the  $\pi^+$  in the center of mass frame. Since the overall number of events is fitted we can absorb  $\alpha_1$  into the normalization factor  $N$  and thus we set  $\alpha_1 = 1$ .

*Fit results and discussion.*— We fit the amplitudes to the  $D^0 D^0 \pi^+$  invariant mass spectrum using MINUIT [32] and find a unique solution with desired physical properties. The parameters of the fit are given in Table I, and correspond to  $\chi_{\text{d.o.f}}^2 = 0.95$ . Notice that the error of the parameters from MINUIT is much smaller than that from bootstrap. The comparison between the data and

$K_{11} = 0.007905 \pm 0.006404^{+0.034727}_{-0.082606}$
$K_{12} = K_{21} = 0.5315 \pm 0.0025^{+0.0320}_{-0.0666}$
$K_{22} = 1.4271 \pm 0.0016^{+0.0222}_{-0.0491}$
$\alpha_2 = -0.3215 \pm 0.0015^{+0.0270}_{-0.0606}$
$N_a = 1339.6 \pm 117.7^{+639.1}_{-952.5} \text{ GeV}^{-2}$
$N_b = 568.5 \pm 52.0^{+268.4}_{-394.8} \text{ GeV}^{-2}$
$\chi_{\text{d.o.f}}^2 = 0.95$

TABLE I. Parameters of the best fit, as explained in the text. The  $K$ -matrix elements and production parameters,  $\alpha_i$  are dimensionless. The first uncertainty of the parameters is given from MINUIT, and the second (up and down) uncertainty is from bootstrap within  $2\sigma$ .  $N_a$  is the normalization factor for the data in the full range, while  $N_b$  is for the data in the region of  $T_{cc}^+$ .

the model is shown in Fig. 1. As can be seen, our amplitudes fit the data rather well. To study the resonance we also enlarge the plot of our solution around the  $T_{cc}^+$ , multiplying  $N_b$  instead of  $N_a$  in Eq. (5), as shown in Fig. 2. Once the  $D^0 D^0 \pi^+ - D^0 D^{*+}$  amplitudes are determined on the real axis they can be analytically continued to extract the information about the singularities located on the nearby Riemann sheets (RS). These are reached from the real  $s$ -axis though the unitary cuts of the  $C_i(s)$  functions. Near the pole  $s_R$  residues/couplings in  $n$ -th RS are computed from

$$T_{ij}^n(s) \simeq \frac{g_i^n g_j^n}{s_R^n - s}. \quad (6)$$

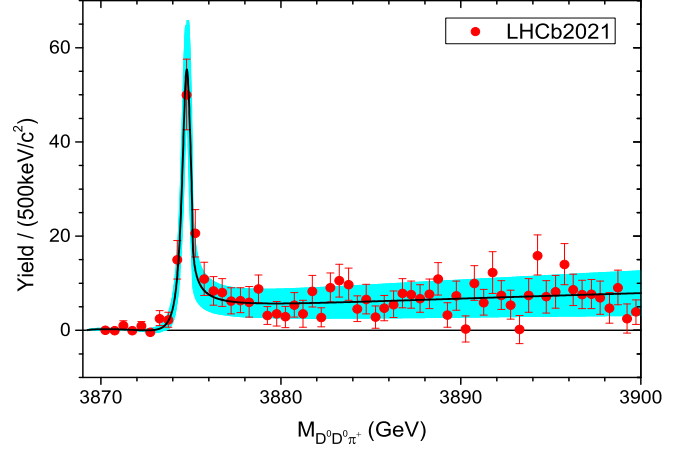


FIG. 1. Fit to the  $D^0 D^0 \pi^+$  invariant mass spectrum. The LHCb 2021 data is from Ref. [18, 19]. The cyan bands are taken from bootstrap within  $2\sigma$ .

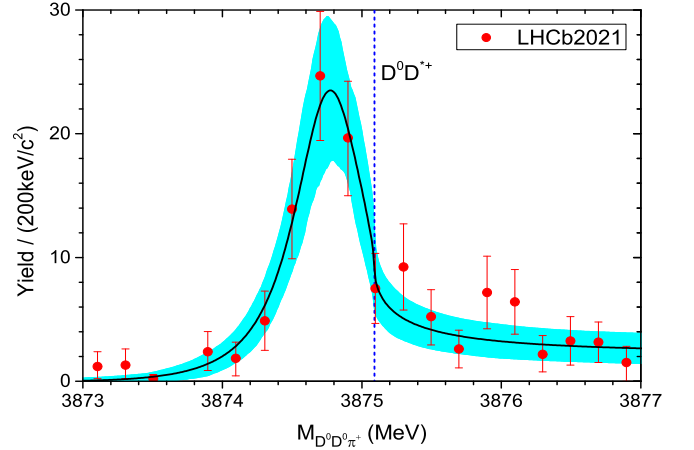


FIG. 2. Fit to the  $D^0 D^0 \pi^+$  invariant mass spectrum around the  $T_{cc}^+$ . The cyan bands are taken from bootstrap method within  $2\sigma$ .

We find a single pole on RS-II and the pole parameters are given in Table II. Here we follow the standard labeling of the sheets, *e.g.* the second sheet is reached from the physical region by moving into the lower complex plane between two thresholds [33]. The uncertainty of the pole parameters come from bootstrap within  $2\sigma$ .

Notice that in the bootstrap method, where the data points are varied randomly, all the poles are located in RS-II. Since  $|g_2| > |g_1|$  it appears that  $T_{cc}^+$  couples more strongly (roughly a factor of three) to the  $D^0 D^{*+}$  channel than to the  $D^0 D^0 \pi^+$  channel. This supports the hypothesis that  $T_{cc}^+$  is a composite object dominated by the  $D^0 D^{*+}$  component.

The trajectory of the pole on the second Riemann sheet is studied by varying  $\lambda$  which is introduced to modify the strength of coupling between the two channels,  $K_{12}(s) \rightarrow \lambda K_{12}(s)$ , so that  $\lambda = 1$  corresponds to the physical amplitude while for  $\lambda = 0$ , Eq.(1) represents two uncoupled channels. As a function of  $\lambda$  the pole

pole location (MeV)	$g_{D^0 D^0 \pi^+}^{II} =  g e^{i\varphi}$		$g_{D^0 D^{*+}}^{II} =  g e^{i\varphi}$	
	$ g_1 $ (GeV)	$\varphi_1$ (°)	$ g_2 $ (GeV)	$\varphi_2$ (°)
$3874.75^{+0.12}_{-0.06} - i 0.34^{+0.06}_{-0.12}$	$0.23^{+0.03}_{-0.04}$	$10^{+13}_{-9}$	$0.70^{+0.03}_{-0.03}$	$11^{+13}_{-8}$

TABLE II. The pole location and its residues (both magnitude and phase) from our fit, in RS-II.

trajectory is shown in Fig. 3. As  $\lambda$  decreases, the pole

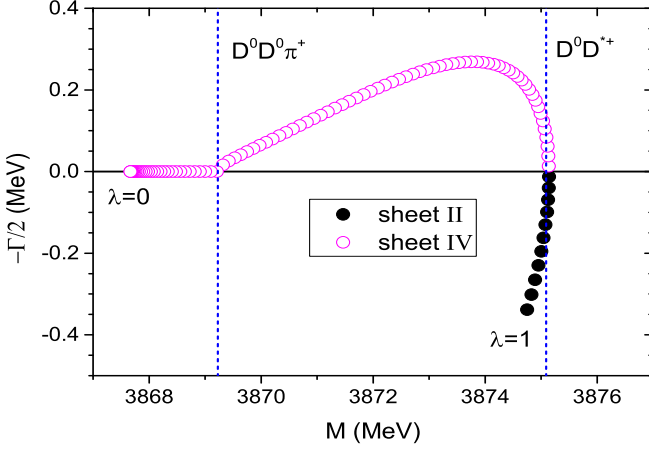


FIG. 3. The trajectories of pole locations by varying  $\lambda$ . The black filled circles are the poles in the second Riemann sheet,  $1 \geq \lambda \geq 0.90$ , and the magenta open circles are the poles in the fourth Riemann sheet,  $0.89 \geq \lambda \geq 0$ , respectively. The step of  $\Delta\lambda$  is 0.01.

moves upwards from the lower half  $\sqrt{s}$ -plane of RS-II to the upper half plane of RS-IV, crossing the real axis above the second (heavier)  $D^0 D^{*+}$  threshold. This does not violate unitarity since while moving from the second to the fourth sheet the pole never crosses the physical region. As this happens the resonance bump seen on the real axis between thresholds moves towards the heavier threshold and as the pole enters the fourth sheet it becomes a cusp. As  $\lambda$  is decreased further the poles moves below the lower threshold and into the real axis. Finally it reaches the mass just  $\sim 1.5$  MeV below the  $D^0 D^0 \pi^+$  threshold. Notice that at the end of the trajectory with  $\lambda = 0$ , corresponding to the  $D^0 D^{*+}$  single channel, the pole in the real axis below threshold is a virtual state. This implies that in the absence of channel coupling the  $D^0 D^{*+}$  system may not be sufficiently attractive to produce a molecule. If so the  $T_{cc}^+$  is not a true bound state (a pole remaining on the second sheet) but an effect of a complicated interplay of weak attraction and channel interactions. This behaviour is similar to that of the  $P_c(4312)$ , which was found to be likely an effect of weak interaction between  $\Sigma_c^+ \bar{D}^0$  and coupling the the  $J/\psi p$  channel [34].

*Role of the  $D^*$  width.*— Since  $D^{*+}$  is unstable its contribution to the spectral function corresponds to a branch cut (below the real axis) and not a pole. To account for that we modify the Chew-Mandelstam  $C_2$  accordingly

[35]:

$$C_2(s) \rightarrow \frac{1}{\pi} \int_{s_{tr, D\pi}}^{\infty} ds' C(s; \sqrt{s'}, m_2) \text{Im} f_{D\pi}(s') \quad (7)$$

with  $s_{th, D\pi} = (M_{D^0} + m_{\pi^+})^2$  being the threshold for the reaction  $D^0 \pi^+ \rightarrow D^{*+} \rightarrow D^0 \pi^+$  and  $f_{D\pi}(s) = D^{-1}(s)$ , the scattering amplitude in the single resonance approximation, with  $D(s) = \tilde{M}^2 - s - \Sigma(s)$ , and  $\Sigma(s) = g^2(s - s_{th, D\pi})C(s; M_2, m_2)$  so that the imaginary part,  $\text{Im}\Sigma(s) = g^2(s - s_{th, D\pi})\rho_2(s)$  is the energy dependent width corresponding to the  $P$ -wave decay of the  $D^{*+} \rightarrow D^0 \pi^+$ . With the parameters  $g = 0.4451$  and  $\tilde{M} = 2010.77$  MeV the amplitude  $f$  reproduces the line shape of the  $D^*$  correspond to a Breit-Wigner resonance with pole at  $M_{D^{*+}} - i\Gamma_{M_{D^{*+}}}/2 = 2010.26 - i0.04$  MeV. With this modification of  $C_2(s)$ , we fit the coupled channel amplitudes again and find a rather similar solution to the previous one. A pole is found in RS-II with  $3874.76^{+0.08}_{-0.04} - i 0.34^{+0.02}_{-0.10}$  MeV, and the residues are extracted as  $|g_1| = 0.22^{+0.01}_{-0.04}$  GeV and  $|g_2| = 0.71^{+0.01}_{-0.05}$  GeV. Even the pole trajectory is the same as what we found in Fig.3, with only the pole moves towards but not reach the real axis. Also the destination of the pole (with  $\lambda = 0$ ) being roughly 1.6 MeV above the  $D^0 D^0 \pi^+$  threshold. These support the conclusion before.

*Summary.*— In this letter we performed amplitude analysis on the invariant mass spectrum of  $D^0 D^0 \pi^+$ . The  $D^0 D^0 \pi^+ - D^0 D^{*+}$  coupled channel scattering amplitude is constructed using a K-matrix within the Chew-Mandelstam formalism. Then we apply the Au-Morgan-Pennington method to study the final state interactions for the invariant mass spectrum of  $D^0 D^0 \pi^+$ . A high quality fit to the experiment data of LHCb [18, 19] is obtained. We find a pole in the second Riemann sheet for the  $T_{cc}^+$ , with the pole location  $3874.75^{+0.12}_{-0.06} - i 0.34^{+0.06}_{-0.12}$  MeV. By reducing the strength of inelastic channels we obtain the pole trajectory that suggests  $T_{cc}$  might be a  $D^0 D^{*+}$  virtual state. Precise measurements of the line shape would be need to further reduce theoretical uncertainties.

*Acknowledgements.*— This work is supported by Joint Large Scale Scientific Facility Funds of the National Natural Science Foundation of China (NSFC) and Chinese Academy of Sciences (CAS) under Contract No.U1932110, National Natural Science Foundation of China with Grants No.11805059, No.11805012, No.11675051 and No.12061141006, Fundamental Research Funds for the central universities of China, and U.S. Department of Energy Grants No. DE-AC05-06OR23177 and No. DE-FG02-87ER40365.

\* dailingyun@hnu.edu.cn

† aszczepa@indiana.edu

<sup>†</sup> yujiesheng@hnu.edu.cn

- [1] Murray Gell-Mann. A Schematic Model of Baryons and Mesons. *Phys. Lett.*, 8:214–215, 1964.
- [2] G. Zweig. An SU(3) model for strong interaction symmetry and its breaking. Version 1. CERN-TH-401 . 1964.
- [3] G. Zweig. *An SU(3) model for strong interaction symmetry and its breaking. Version 2. Developments in the quark theory of hadrons, vol.1, 1964 - 1978.* 1964.
- [4] S. K. Choi et al. Observation of a narrow charmonium - like state in exclusive  $B^{+-} \rightarrow K^{+-} \pi^+ \pi^- J/\psi$  decays. *Phys. Rev. Lett.*, 91:262001, 2003.
- [5] T. Aaltonen et al. Evidence for a Narrow Near-Threshold Structure in the  $J/\psi\phi$  Mass Spectrum in  $B^+ \rightarrow J/\psi\phi K^+$  Decays. *Phys. Rev. Lett.*, 102:242002, 2009.
- [6] A. Bondar et al. Observation of two charged bottomonium-like resonances in  $\Upsilon(5S)$  decays. *Phys. Rev. Lett.*, 108:122001, 2012.
- [7] M. Ablikim et al. Observation of a Charged Charmoniumlike Structure in  $e^+e^- \rightarrow \pi^+\pi^- J/\psi$  at  $\sqrt{s}=4.26$  GeV. *Phys. Rev. Lett.*, 110:252001, 2013.
- [8] M. Ablikim et al. Observation of a Charged Charmoniumlike Structure  $Z_c(4020)$  and Search for the  $Z_c(3900)$  in  $e^+e^- \rightarrow \pi^+\pi^- h_c$ . *Phys. Rev. Lett.*, 111(24):242001, 2013.
- [9] M. Ablikim et al. Observation of a charged charmoniumlike structure in  $e^+e^- \rightarrow (D^*\bar{D}^*)^\pm \pi^\mp$  at  $\sqrt{s}=4.26$  GeV. *Phys. Rev. Lett.*, 112(13):132001, 2014.
- [10] Victor Mukhamedovich Abazov et al. Search for the  $X(4140)$  state in  $B^+ \rightarrow J/\psi\phi K^+$  decays with the D0 Detector. *Phys. Rev. D*, 89(1):012004, 2014.
- [11] Serguei Chatrchyan et al. Observation of a Peaking Structure in the  $J/\psi\phi$  Mass Spectrum from  $B^\pm \rightarrow J/\psi\phi K^\pm$  Decays. *Phys. Lett. B*, 734:261–281, 2014.
- [12] Roel Aaij et al. Observation of  $J/\psi\phi$  structures consistent with exotic states from amplitude analysis of  $B^+ \rightarrow J/\psi\phi K^+$  decays. *Phys. Rev. Lett.*, 118(2):022003, 2017.
- [13] Roel Aaij et al. A model-independent study of resonant structure in  $B^+ \rightarrow D^+ D^- K^+$  decays. *Phys. Rev. Lett.*, 125:242001, 2020.
- [14] Roel Aaij et al. Amplitude analysis of the  $B^+ \rightarrow D^+ D^- K^+$  decay. *Phys. Rev. D*, 102:112003, 2020.
- [15] Feng-Kun Guo, Christoph Hanhart, Ulf-G. Meißner, Qian Wang, Qiang Zhao, and Bing-Song Zou. Hadronic molecules. *Rev. Mod. Phys.*, 90(1):015004, 2018.
- [16] Yan-Rui Liu, Hua-Xing Chen, Wei Chen, Xiang Liu, and Shi-Lin Zhu. Pentaquark and Tetraquark states. *Prog. Part. Nucl. Phys.*, 107:237–320, 2019.
- [17] Nora Brambilla, Simon Eidelman, Christoph Hanhart, Alexey Nefediev, Cheng-Ping Shen, Christopher E. Thomas, Antonio Vairo, and Chang-Zheng Yuan. The XYZ states: experimental and theoretical status and perspectives. *Phys. Rept.*, 873:1–154, 2020.
- [18] Franz Muheim, on behalf of the LHCb Collaboration, LHCb highlights. *talk at European Physical Society conference on high energy physics*, 2021.
- [19] Liupan An, on behalf of LHCb collaboration, Experimental review of hidden-charm states. *talk at HADRON2021*, 2021.
- [20] L. Y. Dai, Meng Shi, Guang-Yi Tang, and H. Q. Zheng. Nature of  $X(4260)$ . *Phys. Rev. D*, 92(1):014020, 2015.
- [21] Xian-Wei Kang, Bastian Kubis, Christoph Hanhart, and Ulf-G. Meißner.  $B_{14}$  decays and the extraction of  $|V_{ub}|$ . *Phys. Rev. D*, 89:053015, 2014.
- [22] Ling-Yun Dai and Michael R. Pennington. Comprehensive amplitude analysis of  $\gamma\gamma \rightarrow \pi^+\pi^-, \pi^0\pi^0$  and  $\bar{K}K$  below 1.5 GeV. *Phys. Rev. D*, 90(3):036004, 2014.
- [23] I. V. Danilkin, C. Fernández-Ramírez, P. Guo, V. Mathieu, D. Schott, M. Shi, and A. P. Szczepaniak. Dispersive analysis of  $\omega/\phi \rightarrow 3\pi, \pi\gamma^*$ . *Phys. Rev. D*, 91(9):094029, 2015.
- [24] Yun-Hua Chen, Martin Cleven, Johanna T. Daub, Feng-Kun Guo, Christoph Hanhart, Bastian Kubis, Ulf-G. Meißner, and Bing-Song Zou. Effects of  $Z_b$  states and bottom meson loops on  $\Upsilon(4S) \rightarrow \Upsilon(1S, 2S)\pi^+\pi^-$  transitions. *Phys. Rev. D*, 95(3):034022, 2017.
- [25] De-Liang Yao, Ling-Yun Dai, Han-Qing Zheng, and Zhi-Yong Zhou. A review on partial-wave dynamics with chiral effective field theory and dispersion relation. *Rept. Prog. Phys.*, 84(7):076201, 2021.
- [26] P. A. Zyla et al. Review of Particle Physics. *PTEP*, 2020(8):083C01, 2020.
- [27] Geoffrey F. Chew and Stanley Mandelstam. Theory of low-energy pion pion interactions. *Phys. Rev.*, 119:467–477, 1960.
- [28] Bonnie J. Edwards and Gerald H. Thomas. Inelastic thresholds and dibaryon resonances. *Phys. Rev. D*, 22:2772, 1980.
- [29] Shi-Qing Kuang, Ling-Yun Dai, Xian-Wei Kang, and De-Liang Yao. Pole analysis on the hadron spectroscopy of  $\Lambda_b \rightarrow J/\psi p K^-$ . *Eur. Phys. J. C*, 80(5):433, 2020.
- [30] K.L. Au, D. Morgan, and M.R. Pennington. Meson dynamics beyond the quark model: A study of final state interactions. *Phys. Rev. D*, 35:1633, 1987.
- [31] Ling-Yun Dai and M. R. Pennington. Two photon couplings of the lightest isoscalars from BELLE data. *Phys. Lett. B*, 736:11–15, 2014.
- [32] F. James and M. Roos. Minuit: A System for Function Minimization and Analysis of the Parameter Errors and Correlations. *Comput. Phys. Commun.*, 10:343–367, 1975.
- [33] William R. Frazer and Archibald W. Hendry. S-Matrix Poles Close to Threshold. *Phys. Rev.*, 134:B1307–B1314, 1964.
- [34] C. Fernández-Ramírez, A. Pilloni, M. Albaladejo, A. Jackura, V. Mathieu, M. Mikhasenko, J. A. Silva-Castro, and A. P. Szczepaniak. Interpretation of the LHCb  $P_c(4312)^+$  Signal. *Phys. Rev. Lett.*, 123(9):092001, 2019.
- [35] J. L. Basdevant and Edmond L. Berger. Unstable Particle Scattering and an Analytic Quasiunitary Isobar Model. *Phys. Rev. D*, 19:239, 1979.